

# Influence of foreign Fe ions on wet chemical synthesis of Pt nanoparticle thin films at ambient temperature: *in situ* versus direct addition

Ranjan K. Sahu,<sup>\*a</sup> Debangshu Mukherjee,<sup>b</sup> J. P. Tiwari,<sup>c</sup> T. Mishra,<sup>a</sup> S. K. Roy<sup>b</sup> and L. C. Pathak<sup>a</sup>

Received 22nd April 2009, Accepted 23rd June 2009

First published as an Advance Article on the web 24th July 2009

DOI: 10.1039/b908080e

Novel Pt nanoparticle thin films have been successfully synthesized on glass surfaces *via* a wet chemical method that comprised reduction of aqueous hexachloroplatinic acid solution by ascorbic acid in the presence of hematite ( $\alpha$ -Fe<sub>2</sub>O<sub>3</sub>) at room temperature. Scanning electron microscopy (SEM), transmission electron microscopy (TEM), powder X-ray diffraction (XRD), atomic absorption spectroscopy, X-ray photoelectron spectroscopy (XPS), UV-Vis absorption spectroscopy and a scratch testing method have been used to characterize the final and intermediate products of Pt films. It was found that there existed competition between precipitation of nanoparticles and formation of Pt nanoparticle thin films, which is controlled by the source of foreign Fe ions *i.e.* *in situ* or direct addition of foreign ions. Besides, the negatively charged glass surface and positively charged hematite surface under the synthesis condition of pH  $\sim$ 3 assisted heterogeneous nucleation of Pt on glass surfaces. The measured adhesive strength of the film on glass substrate is 106 Mpa and the density of states overlaps the Fermi energy ( $E_f = 0$ ), indicating the conducting films are strongly bonded on the glass surface. The synthetic protocol outlined here shows a new synthetic route to integrate metal nanoparticles directly on glass substrates.

## Introduction

One of the main challenges in the development of devices utilizing nanoparticles is the integration of nanoparticles onto supporting materials. In particular, the preparation of platinum nanoparticles has received much attention due to their potential applications in advanced devices and systems.<sup>1</sup> Many synthetic protocols have been developed for the assembly of nanoparticles into thin films.<sup>2</sup> In general, liquid phase methods are extremely simple compared to chemical vapor deposition and physical vapor deposition methods for the deposition of any kind of films constituted of nanoparticles. A beaker is enough for the deposition of films *via* a solution method that enables the exploitation of the solution process towards industrial use in order to be cost effective. Indeed Porter *et al.* have shown the formation of Pt films composed of nanoparticles upon various semiconducting or metal substrates such as Ge (100), Cu, Zn and Sn using an electroless method, where the spontaneous reduction of metallic ions to metallic particles occurs in the solution without an external source of electric current, the so-called galvanic displacement reaction.<sup>3</sup> However, emerging technologies such as photo induced activities of Pt by exciting the film from the other side of substrate requires the substrate to be light transparent like glass. Unfortunately, the galvanic displacement reaction does not take place when the substrate is glass which limits the direct

deposition of a Pt film *via* an electroless method. Recently, Yang *et al.* have reported the deposition of a Pt film on a glass substrate that was only possible by precoating a Au layer on glass.<sup>4</sup> To circumvent these problems, it remains a challenge to develop a methodology for the deposition of a Pt film consisting of nanoparticles directly on glass.

In this article, we report a novel room temperature synthesis of Pt nanoparticle thin films on glass substrates directly by reducing the platinum precursor (H<sub>2</sub> [PtCl<sub>6</sub>]) using ascorbic acid ( $E^0_{\text{red}} = 0.076$  V, dibasic acid with  $\text{p}K_{a1} = 4.17$  and  $\text{p}K_{a2} = 11.57$ ) in the presence of hematite ( $\alpha$ -Fe<sub>2</sub>O<sub>3</sub>). Here, hematite acts as a source of foreign element. Addition of foreign elements directly controls the reaction kinetically and leads to the formation of the oxide film on glass directly, which has been observed in the case of ZnO.<sup>5</sup> This direct deposition of films on glass, however, does not occur in the case of Pt. We follow a different approach where the key concept is the *in situ* addition of Fe ions as foreign elements continuously to the reductive solution through dissolution of hematite in ascorbic acid that can suppress the nucleation of Pt kinetically by virtue of the stabilization of Pt (IV) and Pt (II) in the solution and promotes the nucleation on the glass surface. Besides, the induced positive surface charge of hematite (zero point charge is 6.5) and the induced negative charge on the glass surface (zero point charge is 2.5) at pH  $\sim$ 3 would further assist the heterogeneous nucleation.

## Experimental section

### Materials synthesis

Hexachloroplatinic acid (H<sub>2</sub> [PtCl<sub>6</sub>]), ascorbic acid and hematite were obtained from Sigma-Aldrich, Rankem India and Merck, respectively. All chemicals used were of analytical grade.

<sup>a</sup>Materials Science & Technology Division, National Metallurgical Laboratory, CSIR, Jamshedpur-831007, India. E-mail: rksahu@nmlindia.org

<sup>b</sup>Department of Metallurgical and Materials Engineering, Indian Institute of Technology, Kharagpur-721302, India

<sup>c</sup>Functional Materials Division, Central Electrochemical Research Institute, CSIR, Karaikudi-630006, India

Platinum thin films composed of nanoparticles were synthesized by reducing hexachloroplatinic acid (HCPA) with ascorbic acid ( $C_6H_6O_6$ ) in the presence of foreign Fe ions using source hematite ( $\alpha\text{-Fe}_2\text{O}_3$ ) at room temperature. In a typical synthesis, 0.04 g of ascorbic acid was added to 2 ml of aqueous HCPA solution (0.01M). The solution was diluted by adding 10 ml of deionized water. Subsequently, 0.2 g of  $\alpha\text{-Fe}_2\text{O}_3$  (particle size  $\sim 0.6\ \mu\text{m}$ ) was added to the solution and the reaction vessel sealed. The pH of the solution was measured to be 3.0. It was observed that the coating of Pt film on the surface of glass bottle started after 4 h, which clearly appeared as black spots on the glass surface. For coatings of Pt films on flat glass slides, the glass slide was placed vertically inside the bottle. In order to evaluate the role of foreign Fe ions, we also carried out the reduction of HCPA in ascorbic acid by adding  $\text{FeCl}_3$  as a source of Fe ions instead of  $\alpha\text{-Fe}_2\text{O}_3$ . Besides, we varied the concentration of HCPA while keeping other experimental parameters constant to understand the growth process of the Pt film.

### Characterization

The Fe concentration during the dissolution process was detected using an atomic absorption spectroscopic (AAS) technique. SEM images were taken using a JEOL microscope operated at an acceleration voltage in the range 5–20 kV. The selected area electron diffraction (SAED) pattern of the Pt films was taken using the JEOL 3010 transmission electron microscope. The UV-Vis spectra were obtained using a Shimadzu UV-2550 spectrophotometer. XRD patterns were recorded using Bruker (D8 DISCOVER) diffractometer equipped with a  $\text{Co K}\alpha$  radiation source. X-Ray photoelectron spectrometer (XPS) measurements with an Al  $\text{K}\alpha$  monochromatized X-ray source ( $E = 1486.6\ \text{eV}$ ). The instrument was operated at a pressure of  $6 \times 10^{-9}$  Torr in the analysis chamber. The X-ray spot had an elliptical shape with a short axis of  $500\ \mu\text{m}$  when focused on the surface. Photoelectrons were collected with pass energy of 80 eV for surveys, and 20 eV for high-resolution spectra. The binding energies were collected with a reference to the maximum intensity of the C 1s (285.0 eV). Analysis of the spectra was done using CASA XPS software. The adhesion of the films to the glass surface was determined by a scratch testing method using a Scratch Tester (DUCOM, Tr 101). The adhesion strength is calculated based on the approximation equation,  $\sigma = 2kL_c/\pi R_d$ , where  $L_c$  is critical load (5N),  $k$  is coefficient (1),  $R$  is radius of scratching point (0.2 mm) and  $d$  is scratch width ( $150\ \mu\text{m}$ ).<sup>6</sup> The load at which the change in slope of tractional force occurs abruptly, called critical load.

### Results and discussion

Fig. 1 summarizes all the steps and observations involved in the growth of the Pt films on glass substrates. The color of aqueous HCPA solution changes from yellow (I) to black (II) by the addition of ascorbic acid (AA). The appearance of a color change indicates the formation of Pt. The Pt particles settle down at the bottom of glass bottle after 30 min. To control the nucleation of Pt by adding foreign ions, the same reaction was carried out in the presence of  $\text{FeCl}_3$  as a source of Fe ion. It was observed that the solution color becomes black with the formation of the Pt

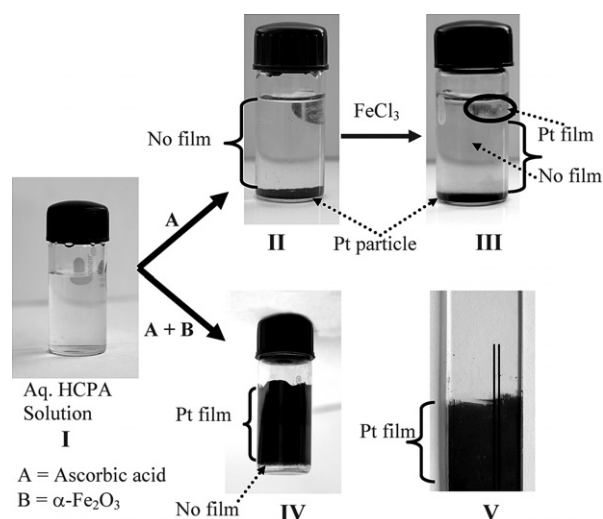


**Fig. 1** View of aqueous HCPA solution (I) produces Pt particles (II) with the addition of ascorbic acid. Addition of 10 ppm  $\text{FeCl}_3$  to the reductive solution assists the formation of a Pt film in a small region (III) only. However, the dissolution of  $\alpha\text{-Fe}_2\text{O}_3$  assists the formation of a Pt film on the glass bottle (IV) and on the glass slide (V).

film only in a small region (III). Like the previous observation, the black Pt particles settle at the bottom after 30 min. However, with the addition of  $\alpha\text{-Fe}_2\text{O}_3$  as a source of Fe ions, the Pt nanoparticles were deposited on the wall of the glass bottle (IV) as well as on the vertically placed glass slide (V) that was inside the bottle. These observations suggest that the source of Fe ions plays a key role in controlling nucleation of the Pt nanoparticles onto the glass substrate.

SEM images of the Pt films obtained by varying the HCPA concentration (Fig. 2) reveal that the film is formed *via* layer-by-layer deposition. Each layer consists of spherical

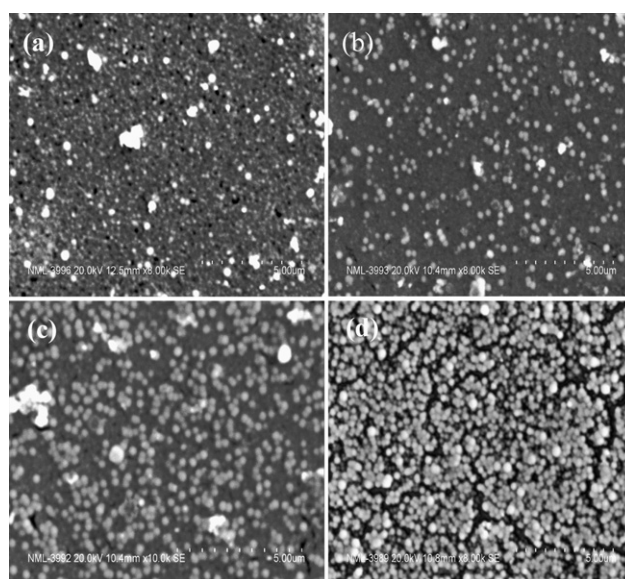


**Fig. 2** SEM images of Pt films obtained from different HCPA concentrations; (a) 0.02 M (b) 0.03 M (c) 0.04 M (d) 0.05 M after 6 h of reaction while keeping other experimental parameters constant.

nanoparticles of 150 nm size and the next layer is formed by adsorption of nanoparticles due to the autocatalytic nature of Pt. However, the observation of few holes in the layer structures, indicating the second layer grows on top of the first layer before the first layer is covered fully.

Fig. 3a shows the XRD pattern of a Pt nanoparticle thin film that can be indexed to FCC structure with {111}, {200}, {220} and {311} diffractions. This is also supported by the SAED pattern of the sonicated Pt film, indicating a single phase of Pt (Fig. 3b). The film was further characterized using XPS. The XPS spectra of the  $4f_{5/2}$  and  $4f_{7/2}$  peaks of the Pt films appeared at 74.7 eV and 71.53 eV, respectively with an asymmetric nature, corresponding to the Pt (0) state (Fig. 3c). After the deconvolution of XPS spectra, the additional peaks appear at 75.1 eV and 71.94 eV for respective  $4f_{5/2}$  and  $4f_{7/2}$  binding energies. The additional peaks could arise due to the existence of other phases of Pt, where the valency state of Pt is +2 or +4. However, the energy shift is much lower than the value observed when Pt is in the +2 valence state ( $\Delta E = 1.6$  eV) or the +4 valence state ( $\Delta E = 2.8$  eV) with respect to the Pt (0) state. It is also much lower than the value observed when the Pt nanoparticles are partially oxidized.<sup>7</sup> The other probable reason is that the asymmetric nature of the Pt 4f peak could arise due to the chemical interaction between the Pt surface and the ligands (ascorbate ion and chloride ion), where the binding energy of Pt (0) increases if the Pt atoms act as electron donors or decreases if the Pt atoms act as electron acceptors. In such a case the XPS spectrum would arise from both the surface effect as well as bulk effect and it is expected to be of an asymmetric nature. Therefore, the result of high resolution XPS Pt (4f) spectra using depth profile analysis mode would provide valuable information to understand the possible reasons pertaining to charge transfer between metal and ligand

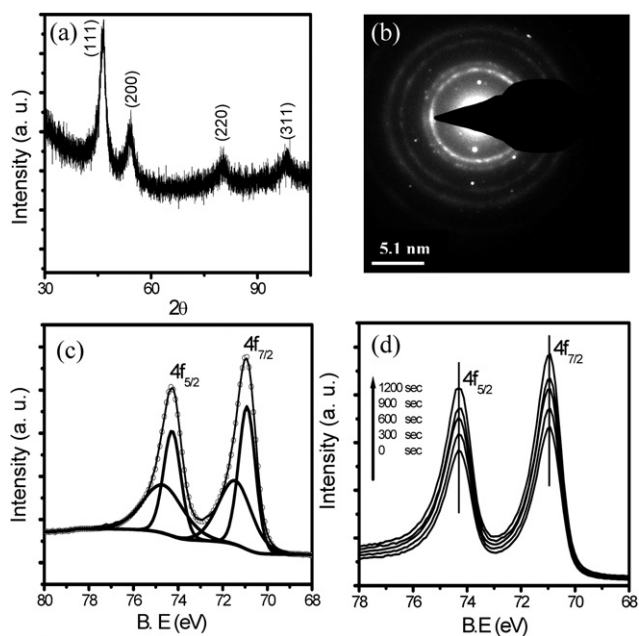


**Fig. 3** (a) XRD of a Pt film; (b) SAED pattern of a Pt film; (c) XPS data of a Pt film (d) XPS data of a Pt (4f) using depth profile analysis mode showing the position as well as shape of the peaks that remained the same even after etching the surface at different time intervals.

that profoundly affect the symmetry of Pt 4f peak. However, the shape of Pt peak remains same after etching the surface at different time intervals (Fig. 3d). The depth profile analysis measurement suggests that the asymmetric effect of the peak does not arise from the charge transfer of ligand. These results indicate that Pt nanoparticles are not attached with the ascorbate or chloride ion. Therefore, the observable asymmetric nature of the peak can be attributed to the electron-hole excitation near Fermi level<sup>8</sup> since the films are conducting at room temperature.

To know the quality of film prepared *via* wet chemical method with respect to adhesiveness and conductivity, the adhesive properties and density of states of the films were measured at room temperature. The scratch testing method revealed that the films have an adhesive strength of 106 Mpa (Fig. 4), indicating the room temperature deposited Pt films have good adherence properties with the glass surface. The photoelectron spectroscopy studies of the Pt film at  $T = 300$  K show that the density of states overlaps the Fermi energy level ( $E_f = 0$  eV). The strong spectral weight near the Fermi energy indicates the film is highly conducting. These results suggest that good bonding strength with conducting films can be deposited by using the present protocol for the deposition of Pt films *via* a wet chemical method.

It is important to study the dissolution of  $\alpha$ - $\text{Fe}_2\text{O}_3$  in detail in order to understand the role of a foreign ion source. To determine the dissolution rate of  $\alpha$ - $\text{Fe}_2\text{O}_3$  in ascorbic acid, we have carried out a blank experiment without HCPA. The solution collected at different time intervals during the dissolution of  $\alpha$ - $\text{Fe}_2\text{O}_3$  in ascorbic acid characterized using an atomic

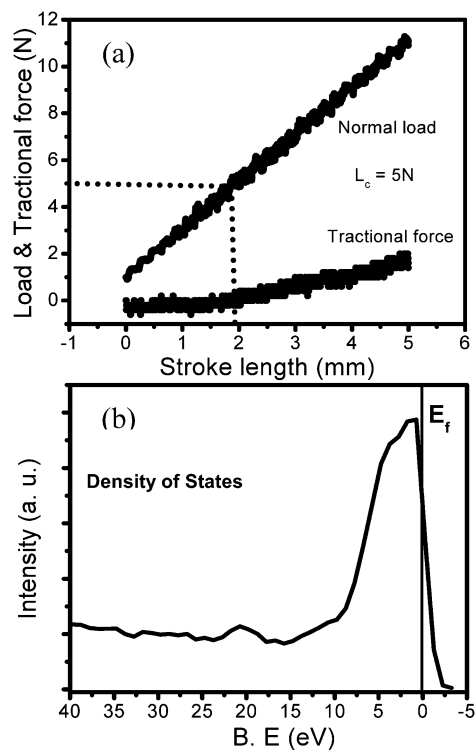


**Fig. 4** (a) Load and tractional force as a function of stroke length of the Pt film. The calculated adhesive strength using the approximation equation is 106 Mpa. (b) Valence band spectra of a Pt film measured at room temperature using XPS technique.

absorption spectroscopy technique (Fig. 5a). This suggests that the dissolution of  $\alpha$ -Fe<sub>2</sub>O<sub>3</sub> in ascorbic acid is very slow, 6 ppm at 4 h, and continuously generates the Fe ion. Initially the rate of dissolution is high and it suppresses in a later stage. The continuous dissolution of  $\alpha$ -Fe<sub>2</sub>O<sub>3</sub> in a reductive solution until the end of the reaction is analogous to the continuous addition of Fe ions to the reaction solution from one side of a container. Whereas, the addition of FeCl<sub>3</sub> as a source of Fe ions, wherein the Fe ions generate through the ionization of FeCl<sub>3</sub> in aqueous solution, is considered to be a direct addition of a constant amount of Fe ions to the solution. The slow addition of a foreign element controls the reaction kinetically, as a result, the impact of  $\alpha$ -Fe<sub>2</sub>O<sub>3</sub> addition is different than FeCl<sub>3</sub>.

To address the role of a foreign Fe ion source in controlling the kinetics of Pt nanoparticle nucleation, we have recorded the UV-Vis spectra of reaction solutions taken at different time intervals of HCPA/AA/ $\alpha$ -Fe<sub>2</sub>O<sub>3</sub> (Fig. 5b) and compared them with the spectra of all the possible combinations of precursor, reducing agent and foreign element: (a) ascorbic acid (AA), HCPA and solution after dissolution of  $\alpha$ -Fe<sub>2</sub>O<sub>3</sub> in ascorbic acid (inset) (b) HCPA/AA (c) HCPA/AA/FeCl<sub>3</sub> (10 ppm) and (d) HCPA/AA/FeCl<sub>3</sub> (30 ppm) (Fig. 6). The peak positions are listed in Table 1. The significant difference in the spectra was observed when the source of the foreign element is  $\alpha$ -Fe<sub>2</sub>O<sub>3</sub>. It can be noted from the UV-Vis data that the reduction process takes more than 5 h to complete in the presence of  $\alpha$ -Fe<sub>2</sub>O<sub>3</sub>, whereas the reaction completes at less than 1 h in the presence of FeCl<sub>3</sub>.

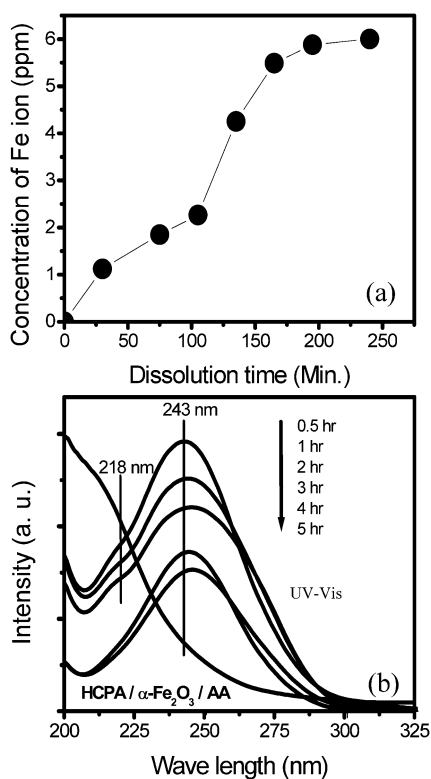


**Fig. 5** (a) Concentration of Fe ions as a function of time during the dissolution of  $\alpha$ -Fe<sub>2</sub>O<sub>3</sub> in ascorbic acid measured by atomic absorption spectroscopy. (b) UV-Vis spectra of the reaction solution comprising HCPA/ $\alpha$ -Fe<sub>2</sub>O<sub>3</sub>/AA taken at different time intervals.

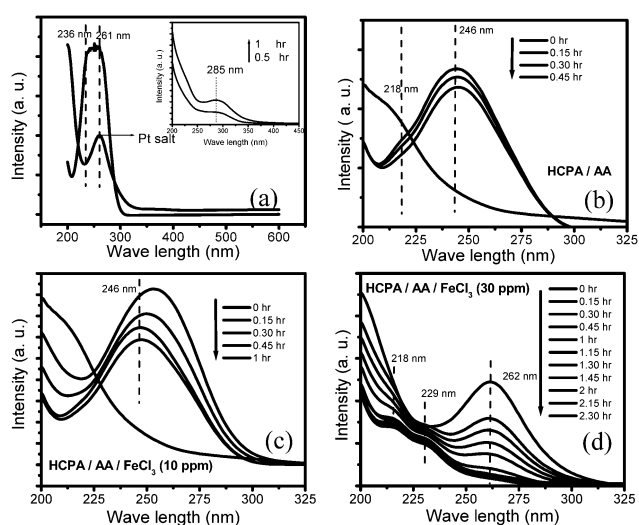


**Fig. 6** UV-Vis spectra of reaction solutions taken at different stages of the synthesis: (a) ascorbic acid (AA), HCPA, and solution after dissolution of  $\alpha$ -Fe<sub>2</sub>O<sub>3</sub> in ascorbic acid (inset) (b) HCPA/AA (c) HCPA/AA/FeCl<sub>3</sub> (10 ppm) and (d) HCPA/AA/FeCl<sub>3</sub> (30 ppm).

**Table 1** Observed absorption position of Pt and ascorbic acid in UV-Vis experiments. These values are verified with the earlier reported data

Wave length position (nm)	Assignment	Reference
236–261	Asc, Asc <sup>-1</sup> , Asc <sup>-2</sup>	1
218, 261	Pt (IV)	2
218, 246	Pt (II)/Pt (IV)	2
218, 229	Pt (II)	2
285	Fe (III)–ascorbic acid	

Moreover, it is observed that the concentration of the foreign element also plays a role in controlling the nucleation of Pt nanoparticles. By varying the FeCl<sub>3</sub> concentration the experiments reveal that the Fe ion concentration should not exceed the critical concentration (10 ppm) until the end of the reaction, above which the Fe ion plays a dominant role in the complexation with ascorbic acid instead of the Pt ion. In fact, no Pt nanoparticles nucleate at room temperature when the Fe ion concentration is above 30 ppm (Fig. 6d). This is due to the formation of a strong complex between the Fe ion and ascorbic acid (stability complex constant,  $K = 1.2 \times 10^3$ ), as a result, the reducing action of AA is arrested. We attribute that the slow and continuous generation of the Fe ion by virtue of the dissolution of  $\alpha$ -Fe<sub>2</sub>O<sub>3</sub> in ascorbic acid is responsible to control the reaction kinetically.

The dissolution of  $\alpha$ -Fe<sub>2</sub>O<sub>3</sub> in ascorbic acid at pH  $\sim$ 3 has been studied previously and a general description of the reaction mechanism consists of adsorption of ascorbic acid to an iron surface site, followed by electron transfer and dissolution of the reduced iron (Fe<sup>2+</sup>).<sup>9</sup> The surface hydroxyl groups, due to the protonation of surface oxide in acidic solution, become active sites for the subsequent adsorption of ascorbic acid. XPS is a powerful tool to investigate the adsorption behavior of ligands on the metal surface. We have, therefore, characterized the used  $\alpha$ -Fe<sub>2</sub>O<sub>3</sub> in the reaction using the XPS technique. Depth profile

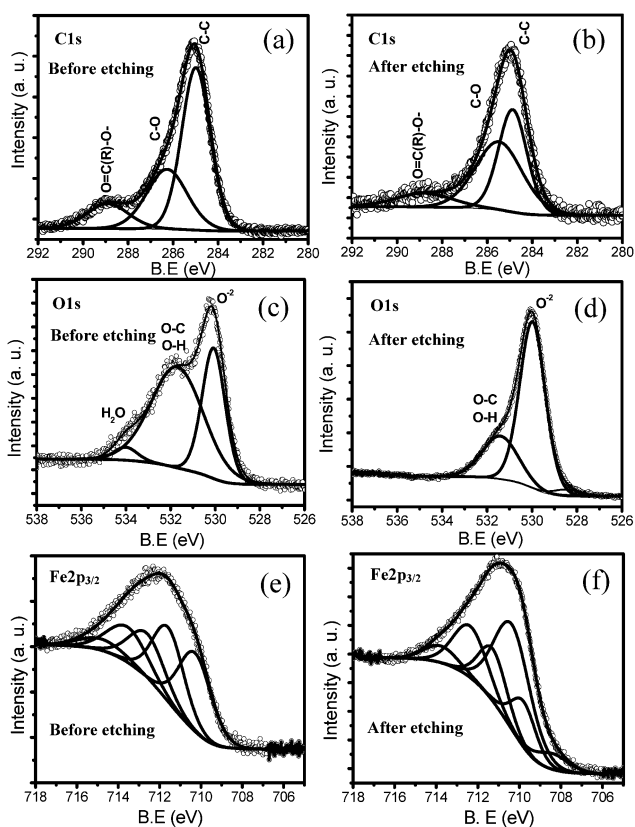


**Fig. 7** High-resolution XPS spectra of C1s, O1s and Fe<sub>2p<sub>3/2</sub></sub> of used  $\alpha$ -Fe<sub>2</sub>O<sub>3</sub> in the reaction and the result compared with the spectra of same  $\alpha$ -Fe<sub>2</sub>O<sub>3</sub> after etching the surface for 40 min.

XPS study of C1s, O1s and Fe<sub>2p<sub>3/2</sub></sub> of  $\alpha$ -Fe<sub>2</sub>O<sub>3</sub> (Fig. 7) shows that the C1s peak consists of three peaks at 285.0 eV, 286.29 eV and 288.83 eV that can be attributed to the C–C or C–H, C–O and O=C(R)–O–, respectively.<sup>10</sup> The appearance of C–O and O=C(R)–O– groups indicate the ascorbic acid has adsorbed onto the surface of  $\alpha$ -Fe<sub>2</sub>O<sub>3</sub>. This also reflects on the O1s spectra of  $\alpha$ -Fe<sub>2</sub>O<sub>3</sub>. The O1s spectra of  $\alpha$ -Fe<sub>2</sub>O<sub>3</sub> show the spectra consists of three different types of peaks corresponding to the structural O<sup>2-</sup>, water (H<sub>2</sub>O) and a broad peak consisting of hydroxyl (OH) group and O–C groups.<sup>10</sup> After etching the sample for 40 min, it is observed that the content of functional groups in the C1s and

O1s decreases and the O1s peak pertaining to water molecule disappears. To understand the association of ascorbic acid onto the surface of  $\alpha$ -Fe<sub>2</sub>O<sub>3</sub>, we have analyzed the Fe2p spectra of used  $\alpha$ -Fe<sub>2</sub>O<sub>3</sub> in detail. The Fe<sub>2p<sub>3/2</sub></sub> is fitted with multiplet four peaks as suggested by Grosvenor for high spin Fe<sup>3+</sup> and a surface peak.<sup>11</sup> The determined binding energy for each peak is listed in Table 2. The significant difference was observed in higher energy peaks, 713.54 eV and 714.85 eV. After etching the sample, the peak at 713.54 eV increased by 0.4 eV and the peak at 714.85 eV disappeared. Besides, two extra peaks (708.54 eV and 709.92 eV) appear at the low binding energy side of Fe<sub>2p<sub>3/2</sub></sub>. The change of observations in the spectra of  $\alpha$ -Fe<sub>2</sub>O<sub>3</sub> after etching the samples can be explained considering the association of ascorbic acid, hydroxyl group due to protonation of  $\alpha$ -Fe<sub>2</sub>O<sub>3</sub> surface and water molecules (Table 2). All these groups attached to the surface of  $\alpha$ -Fe<sub>2</sub>O<sub>3</sub>, which remove after etching the surface. Since the dissolution mechanism of  $\alpha$ -Fe<sub>2</sub>O<sub>3</sub> involved the release of Fe<sup>2+</sup> ions,<sup>9</sup> however, there is no indication of Fe<sup>2+</sup> on the surface of  $\alpha$ -Fe<sub>2</sub>O<sub>3</sub> before etching. The lack of observation of any Fe<sup>2+</sup> suggests that the electrons donated by ascorbic acid to  $\alpha$ -Fe<sub>2</sub>O<sub>3</sub> are delocalized (*i.e.* injected into the conduction band rather than onto a particular site)<sup>12</sup> or the Fe<sup>2+</sup> ion is released from the surface of  $\alpha$ -Fe<sub>2</sub>O<sub>3</sub> to the solution that is assisted by the presence of chloride ion in the solution. Bombardment of  $\alpha$ -Fe<sub>2</sub>O<sub>3</sub> surfaces with Ar<sup>+</sup> ions removes ascorbic acid and concomitantly shows the signature of Fe<sup>2+</sup>. The observed extra peak at 708.54 eV and 709.92 eV after etching corresponds to Fe<sup>2+</sup>. The former one can be attributed to the reduced Fe<sup>2+</sup> caused by bombardment of Ar<sup>+</sup> and the latter can be attributed to the removal of ascorbic acid. One remarkable point should be noted from the depth profile XPS data of Pt film and used  $\alpha$ -Fe<sub>2</sub>O<sub>3</sub> in the reaction that ascorbic acid has a strong ability to form coordination bonds with Fe compared to Pt. Previous studies showed an influence of the organic ligand on the Pt4f binding energy of platinum nanoparticles.<sup>13</sup> The non-appearance of the signature for the ascorbic acid on Pt or glass surfaces and attachment of ascorbic acid on  $\alpha$ -Fe<sub>2</sub>O<sub>3</sub> suggests that positive charge is created on the surface of hematite and negative charge on the surface of glass under the synthesis condition.

There are several mechanisms described in the literature for understanding the growth process of oxide films on glass substrates, which significantly lower the barrier energy for heterogeneous nucleation. This includes; surface of substrate, pH

**Table 2** Binding energies of C1s, O1s and Fe<sub>2p<sub>3/2</sub></sub> of used  $\alpha$ -Fe<sub>2</sub>O<sub>3</sub> in the reaction. Also, the binding energies are given for the same sample after etching for 40 min

	C1s	O1s	Fe <sub>2p<sub>3/2</sub></sub>
Before etching	285 (C–C, C–H)	530.07 (Structural $\alpha$ -Fe <sub>2</sub> O <sub>3</sub> )	710.29 (Main peak)
	286.29 (C–O)	531.70 (O–H, O–C)	711.58
	288.83 (O=C(R)–O)	534.01 (Physio absorbed water)	712.61
After 40 min etching	285 (C–C, C–H)	528.61 (Structural FeO)	713.54
	285.61 (C–O)	530.1 (Structural $\alpha$ -Fe <sub>2</sub> O <sub>3</sub> )	714.85 (Surface peak)
	288.92 (O=C(R)–O)		708.54 (Fe <sup>2+</sup> , FeO)
			709.92 (Fe <sup>2+</sup> )
			710.47 (Main peak)
			711.41
			712.49
			713.92

of the solution, and supersaturation of the solution.<sup>14</sup> The first two factors can be ruled out in our case since they do not change after the addition of  $\alpha$ -Fe<sub>2</sub>O<sub>3</sub> to the solution that is established from the experimental results. Therefore, the film deposition in the solution follows heterogeneous nucleation driven by lowering the degree of supersaturation. This is evident from the UV-Vis experiment (Fig. 5 and 6) as the addition of  $\alpha$ -Fe<sub>2</sub>O<sub>3</sub> delays the reduction of Pt (IV) to Pt (0) to completion. XPS data indicate that the dissolution of iron takes place in the form of Fe<sup>2+</sup> rather than in the form of Fe<sup>3+</sup>. Consequently, redox ionic pairs form between Pt and Fe in the solution by virtue of the close oxidation and reduction potential value Pt (IV)/Pt (II) (0.726 eV)  $\leftrightarrow$  Fe (III)/Fe (II) (0.77 eV). The existence of redox ionic pair reduces the degree of supersaturation and promotes the heterogeneous nucleation. Moreover, the glass wall becomes negatively charged under synthesis conditions (pH  $\sim$ 3) as the isoelectric point of the silicate glass surface is about 2.5. Therefore, negatively charged sites on the glass wall assist preferentially the adsorption of cationic Pt ions and so acted as the heterogeneous nucleation site for the growth of Pt nanoparticles. In a subsequent step, the nucleating object on the glass surface grows by adsorption of the Pt from the solution due to the autocatalytic nature of Pt. UV-Vis experiments revealed that the nucleation rate of the reductive solution in the presence of  $\alpha$ -Fe<sub>2</sub>O<sub>3</sub> is slow as the reaction takes more time to complete. Consequently, the adsorption rate exceeds the nucleation rate, which further favors the Pt film to grow. On the other hand, the nucleation rate is higher than the adsorption rate without  $\alpha$ -Fe<sub>2</sub>O<sub>3</sub> by which the particles form through homogeneous nucleation and settle down at the bottom without forming the Pt film on the glass surface. The protocol for the direct deposition of Pt film on a glass surface shows that the film formation on the glass surface is dependent on the source of foreign element *i.e.* *in situ* or direct addition. This result suggests that controlled nucleation of Pt not only depends on foreign ion but also the way of generating the foreign ion.

In summary, we have demonstrated that the impact of *in situ* addition of foreign Fe ion is different than direct addition in controlling the nucleation of Pt nanoparticles. Using hematite judiciously as a source of Fe ions decreases the supersaturation of the solution that controls the chemical reduction of platinum precursor in an aqueous solution at room temperature. Besides, the induced positive charge on the surface of hematite under the synthetic condition at pH  $\sim$ 3 assists the movement of the cationic platinum ion towards the glass wall of bottle that resulted in the heterogeneous nucleation of Pt nanoparticles. This synthetic process is remarkably simple and it provides a low

temperature facile method for integration of other metallic nanoparticles directly onto glass substrates.

## Acknowledgements

RKS thanks DST, India for financial support under the Project Grant No. SR/FTP/ETA-51/07. This work is partially supported by CSIR network project-NWP 051 on Nanostructured Advanced Materials.

## References

- (a) R. Lenigk, H. Zhu, T.-C. Lo and R. Renneberg, *Fresenius J. Anal. Chem.*, 1999, **364**, 66; (b) M. Matsumiya, W. Shin, N. Izu and N. Murayama, *Sens. Actuators B: Chem.*, 2003, **93**, 309; (c) S. C. Pak, W. Penrose and P. J. Hesketh, *Biosens. Bioelectron.*, 2001, **16**, 371; (d) A. Arora, A. J. de Mello and A. Manz, *Anal. Commun.*, 1997, **34**, 393; (e) K. D. Harris, J. R. McBride, K. E. Nietering and M. J. Brett, *Sens. Mater.*, 2001, **13**, 225; (f) S. Conoci, S. Petralia, P. Samori, F. M. Raymo, S. Di Bella and S. Sortino, *Adv. Funct. Mater.*, 2006, **16**, 1425; (g) B. Stahl, J. Ellrich, N. S. Gajbhiye, G. Wilde, D. Kramer, M. Ghafari, H. Hahn, H. Gleiter, J. Weissmüller, R. Würschum and P. Schlossmacher, *Adv. Mater.*, 2002, **14**, 24; (h) J. Chen, T. Herricks, M. Geissler and Y. Xia, *J. Am. Chem. Soc.*, 2004, **126**, 10854; (i) A. Tao, S. Habas and P. Yang, *Small*, 2008, **4**, 310.
- (a) X. Teng, W. Han, Q. Wang, L. Li, A. I. Frenkel and J. C. Wang, *J. Phys. Chem. C*, 2008, **112**, 14696; (b) T. Nguyen, L. J. Charneski and D. R. Evans, *J. Electrochem. Soc.*, 1997, **144**, 3634; (c) X. M. Xu, J. Liu, Z. Yuan, J. Weaver, C. L. Chen, Y. R. Li, H. Gao and N. Shi, *Appl. Phys. Lett.*, 2008, **92**, 102102; (d) W.-G. Hoi, E.-S. Choi and S.-G. Yoon, *Chem. Vap. Deposition*, 2003, **9**, 321.
- L. A. Porter, H. C. Choi, J. M. Schmeltzer, A. E. Ribbe, L. C. C. Elliott and J. M. Buriak, *Nano Lett.*, 2002, **2**, 1369.
- M.-H. Yang, F.-L. Qu, Y.-S. Lu, G.-L. Shen and R.-Q. Yu, *Talanta*, 2008, **74**, 831.
- M. Kokotov, A. Biller and G. Hodes, *Chem. Mater.*, 2008, **20**, 4542.
- S. K. Mishra and A. S. Bhattacharyya, *Mater. Lett.*, 2008, **62**, 398.
- C. D. Wagner, W. M. Riggs, L. E. Davis, J. F. Moulder, G. E. Muilenberg, *Handbook of X-Ray Photoelectron Spectroscopy*, Perkin-Elmer Corp., Eden Prairie, MN, 1978.
- M. G. Mason, L. J. Gerenser and S. T. Lee, *Phys. Rev. Lett.*, 1977, **39**, 288.
- (a) M. S. Afonso, P. J. Morando, M. A. Blesa, S. Banwart and W. Stumm, *J. Colloid Interface Sci.*, 1990, **138**, 74; (b) R. M. Cornell and U. Schwertmann, *The Iron Oxides*, Wiley-VCH Verlag, GmbH & Co. KGaA, 2nd edn, 2003.
- D. Briggs, *Practical Surface Analysis*, ed., D. Briggs and M. P. Seah, John Wiley, Chichester, 2nd edn, 1992, vol. 1 p. 437.
- A. P. Grosvenor, B. A. Kobe, M. C. Biesinger and N. S. McIntyre, *Surf. Interface Anal.*, 2004, **36**, 1564.
- A. G. Stack, C. M. Eggleston and M. H. Engelhard, *J. Colloid Interface Sci.*, 2004, **274**, 433.
- (a) X. Fu, Y. Wang, N. Wu, L. Gui and Y. Tang, *J. Colloid Interface Sci.*, 2001, **243**, 326; (b) W. Tu, K. Takai, K. Fukui, A. Miyazaki and T. Enoki, *J. Phys. Chem. B*, 2003, **107**, 10134.
- S. Yamabi and H. Imai, *J. Mater. Chem.*, 2002, **12**, 3773.